AMERICAN SOCIETY FOR MICROBIOLOGY | Journal of Virology®

VIRUS-CELL INTERACTIONS

Inhibition of Infectious HIV-1 Production by Rerouting the Cellular Furin Inhibitor Serpin B8

Moritz Petersen,[a] Rishikesh Lotke,[a] Kristina Hopfensperger,[a] Sabina Victoria,[a] Isabell Haußmann,[a] Timo Burster,[b] Hanna-Mari Baldauf,[c] Daniel Sauter[a]

[a]Institute for Medical Virology and Epidemiology of Viral Diseases, University Hospital Tübingen, Tübingen, Germany
[b]School of Sciences and Humanities, Nazarbayev University, Astana, Kazakhstan
[c]Max von Pettenkofer Institute and Gene Center, Virology, National Reference Center for Retroviruses, Faculty of Medicine, LMU Munich, Munich, Germany

ABSTRACT Serpins are a superfamily of proteins that regulate a variety of physiological processes by irreversibly inhibiting the enzymatic activity of different serine proteases. For example, Serpin Family B Member 8 (Serpin B8, also known as PI8 and CAP2) binds to and inhibits the proprotein convertase furin. Like many other viral pathogens, human immunodeficiency virus type 1 (HIV-1) exploits furin for the proteolytic activation of its envelope glycoprotein (Env). Since the furin inhibitor Serpin B8 is expressed in primary target cells of HIV-1 and induced under inflammatory conditions, we hypothesized that it might interfere with HIV-1 Env maturation and decrease infectivity of newly produced virions. Indeed, recombinant Serpin B8 reduced furin-mediated cleavage of an HIV-1 Env reporter substrate *in vitro*. However, Serpin B8 did not affect Env maturation or reduce HIV-1 particle infectivity when expressed in HIV-1-producing cells. Immunofluorescence imaging, dimerization assays and *in silico* sequence analyses revealed that Serpin B8 failed to inhibit intracellular furin since both proteins localized to different subcellular compartments. We therefore aimed at rendering Serpin B8 active against HIV-1 by relocalizing it to furin-containing secretory compartments. Indeed, the addition of a heterologous signal peptide conferred potent anti-HIV-1 activity to Serpin B8 and significantly decreased infectivity of newly produced viral particles. Thus, our findings demonstrate that subcellular relocalization of a cellular protease inhibitor can result in efficient inhibition of infectious HIV-1 production.

IMPORTANCE Many cellular proteases serve as dependency factors during viral infection and are hijacked by viruses for the maturation of their own (glyco)proteins. Consequently, inhibition of these cellular proteases may represent a means to inhibit the spread of viral infection. For example, several studies have investigated the serine protease furin as a potential therapeutic target since this protease cleaves and activates several viral envelope proteins, including HIV-1 Env. Besides the development of small molecule inhibitors, cell-intrinsic protease inhibitors may also be exploited to advance current antiviral treatment approaches. Here, we show that Serpin B8, an endogenous furin inhibitor, can inhibit HIV-1 Env maturation and efficiently reduce infectious HIV-1 production when rerouted to the secretory pathway. The results of our study not only provide important insights into the biology of Serpins, but also show how protein engineering of an endogenous furin inhibitor can render it active against HIV-1.

KEYWORDS Env, Furin, Serpin B8, human immunodeficiency virus

More than 2% of all human genes encode proteases. They represent one of the largest protein families in vertebrates and regulate a plethora of cellular processes, including protein catabolism, signaling cascades, and subcellular trafficking. Intriguingly, cellular proteases are also exploited by a variety of viral pathogens. For example, enveloped viruses, such as the human immunodeficiency virus (HIV), Dengue virus (DENV), or

Editor Guido Silvestri, Emory University

Address correspondence to Daniel Sauter, daniel.sauter@med.uni-tuebingen.de.
The authors declare no conflict of interest.
Received 23 February 2023
Accepted 17 May 2023
Published 5 June 2023

severe acute respiratory syndrome-related coronavirus 2 (SARS-CoV-2) frequently use the serine protease furin (also known as proprotein convertase 3, PCSK3) to activate their envelope glycoproteins (1). Without such a proteolytic activation step, newly formed virions are not or only poorly infectious.

Not surprisingly, protease activity needs to be tightly regulated. One important group of regulators is the protein family of serine protease inhibitors (Serpins). Most Serpins suppress protease activity via an unusual mode of action that involves the formation of covalent Serpin-protease heterodimers (2). This irreversible inhibition is initiated by the binding of the flexible reactive center loop (RCL) of Serpin to the active site of its target protease. Mimicking a substrate, a covalent acyl-enzyme intermediate is formed. In contrast to regular protease substrates, however, Serpins undergo a rapid transition into a lower energy state (S to R transition) that prevents completion of catalysis. Consequently, Serpin remains covalently linked to the target protease, resulting in long-term inactivation of the latter (2).

Although members of the Serpin protein family share a structure, they target a plethora of different proteases. Most Serpins inhibit serine proteases, such as thrombin, cathepsin G, granzyme B, or neutrophil elastase (2). However, some Serpins also act as cross-class inhibitors binding to caspases and other cysteine proteases (2).

Notably, Serpins not only regulate the proteolytic cleavage of cellular substrates, but also contribute to antiviral immune responses by suppressing the proteolytic activation of viral glycoproteins. For example, Serpin E1 (plasminogen activator 1, PAI-1) inhibits cleavage of influenza A virus hemagglutinin by extracellular airway proteases (3). Similarly, proteolytic activation of SARS-CoV-2 Spike is inhibited by Serpins A1 (α1-antitrypsin), C1 (antithrombin) and E1 (4–6). Finally, recent efforts focus on modifying endogenous Serpins to increase their (antiviral) activity and on exploring their therapeutic potential. Mutations in the RCL of Serpin B3, for example, enabled the generation of furin and TMPRSS2 inhibitors that efficiently restrict SARS-CoV-2 replication (7).

Nevertheless, the biological functions of many Serpins remain poorly understood. Since several Serpins are known to be induced and/or released upon interferon (IFN) stimulation or proinflammatory conditions (3, 8, 9), it is tempting to speculate that additional Serpin family members with antiviral activity remain to be discovered. Serpins inhibiting furin may exert particularly broad antiviral activity since this protease is exploited by a plethora of viruses. Screening the scientific literature for Serpins that inhibit furin, we identified Serpin B8 (also called Peptidase inhibitor 8 [PI-8]) as a promising candidate. To the best of our knowledge, this is the only Serpin that has been shown to target furin. Several observations argue for a potential interference of Serpin B8 with furin-mediated maturation of viral proteins: it efficiently inhibits the viral dependency factor furin in cell-free assays (10, 11), it is expressed in a variety of cell types (12, 13), it is induced upon TNF-α stimulation (8, 9), and (like furin) it is released into the extracellular space (11).

Using HIV-1 as a furin-dependent model virus, we therefore aimed at determining basal expression and inducibility of Serpin B8 in primary viral target cells, its effect on furin-mediated cleavage of HIV-1 Env, and a potential inhibition of infectious virion production. We found that Serpin B8 interferes with furin-mediated protein processing *in vitro* but fails to restrict HIV-1 when expressed in virus-producing cells. This lack of inhibition could be ascribed to a lack of colocalization of furin and Serpin B8 inside cells. Importantly, we were able to confer potent antiretroviral activity to Serpin B8 by rerouting it to the secretory pathway. Thus, our findings provide important insights into the biology of Serpin B8 and demonstrate that subcellular relocalization can result in Serpin variants that efficiently reduce infectious HIV-1 production.

RESULTS

Serpin B8 is expressed in primary target cells of HIV-1. Serpin B8 is constitutively expressed in a variety of tissues and cell types, with high expression levels in skin and lymphoid tissues (12, 13). In skin, its expression has been shown to be upregulated by TNF-α stimulation (8, 9), suggesting that it may be involved in immunity and/or

inflammatory processes. Since furin-mediated activation of HIV-1 Env takes place in infected producer cells, we monitored Serpin B8 protein levels in primary $CD4^+$ T cells and monocyte-derived macrophages, the main target cells of HIV-1. Western blot analyses revealed that Serpin B8 is readily detectable in macrophages and expressed at low levels in PHA/IL-2 stimulated $CD4^+$ T cells from healthy donors (Fig. 1A). Infection with different clones of HIV-1 or stimulation with TNF-α did not increase Serpin B8 protein levels in $CD4^+$ T cells. The presence of Serpin B8 in HIV target cells thus raised the possibility that it may affect virion infectivity by interfering with furin-mediated Env processing.

Recombinant Serpin B8 inhibits the proteolytic activity of furin and HIV-1 Env substrate cleavage. Furin recognizes and cleaves polybasic motifs with the consensus sequence R-X-K/R-R (1, 14). To investigate the proteolytic activity of furin in the presence or absence of Serpin B8, we took advantage of a fluorophore-based reporter assay (15). In this approach, cleavage of a coumarin-derived substrate harboring a polybasic cleavage site results in the generation of a fluorescent product (Fig. 1B). Kinetics experiments with a substrate harboring the minimal furin cleavage site R-T-K-R showed a modest, but dose-dependent inhibition of furin activity by recombinant Serpin B8 (Fig. 1C, left panel). A 10-fold molar excess of Serpin B8 over furin reduced substrate cleavage by about 30% (Fig. 1C, right panel). In line with the previously reported role of furin in HIV-1 Env maturation, a substrate harboring the consensus cleavage site of Env (RRVVEREKR) was also cleaved by furin (Fig. 1D, left panel). In this case, Serpin B8 reduced substrate cleavage by up to 60% (Fig. 1D, right panel).

Serpin B8 does not reduce HIV-1 infectivity. Since some Serpins require coactivators to efficiently exert their inhibitor activity (16), we also monitored the effect of Serpin B8 on HIV-1 NL4-3 Env maturation in a cellular environment. Briefly, HEK293T cells were cotransfected with an expression plasmid for HIV-1 Env and increasing amounts of an expression vector for Serpin B8. Untransfected HEK293T cells do not express detectable levels of endogenous Serpin B8 (Fig. 2A). As expected, the immature Env precursor (gp160) was cleaved into its mature forms (gp120/gp41) in the absence of Serpin B8 (Fig. 2A). Surprisingly, overexpression of Serpin B8 did not inhibit Env maturation, but rather slightly enhanced HIV-1 gp160 cleavage.

Since proteolytic cleavage and activation of HIV-1 Env are prerequisites for full virion infectivity, we investigated the effect of Serpin B8 on infectious HIV-1 yield. To this end, HEK293T cells were cotransfected with a proviral construct for HIV-1 NL4-3 and increasing amounts of an expression plasmid for Serpin B8. The previously described furin inhibitor guanylate-binding protein 5 (GBP5) (17) served as a positive control. Two days posttransfection, cell culture supernatants were harvested, and infectious HIV-1 yield was quantified by infecting TZM-GFP reporter cells (18). As expected, GBP5 reduced infectious virus yield in a dose-dependent manner (Fig. 2B, right). In contrast, Serpin B8 had no inhibitory effect, although it was efficiently expressed in the producer cells (Fig. 2B, left). To determine HIV-1 particle infectivity, we normalized total infectivity to the amount of HIV-1 p24 capsid protein in the cell culture supernatants. Again, Serpin B8 showed no reducing activity, while GBP5 significantly decreased relative virion infectivity (Fig. 2C). In line with these findings, Env processing was not inhibited by increasing amounts of Serpin B8 (Fig. 2D). In fact, the percentage of mature gp120 to total Env (i.e., gp120 + gp160) in virions was even slightly enhanced in the presence of Serpin B8. In summary, these findings demonstrate that HIV-1 Env is efficiently processed and activated in cells expressing high levels of Serpin B8.

Serpin B8 does not colocalize with furin. It came as a surprise that Serpin B8 reduced Env cleavage in our *in vitro* protease activity assay (Fig. 1B to D) but did not affect HIV-1 Env maturation when overexpressed in cells (Fig. 2A and D). This raised the possibility that Serpin B8 and furin may not localize to the same subcellular compartments, preventing a direct interaction inside cells. While furin enters the secretory pathway and can be found in the lumen of the ER, Golgi, and secretory vesicles (1), Serpin B8 lacks a signal peptide (Fig. 3A) (19), suggesting that it does not enter the canonical secretory pathway. Previous studies reported a nuclear and/or cytoplasmic

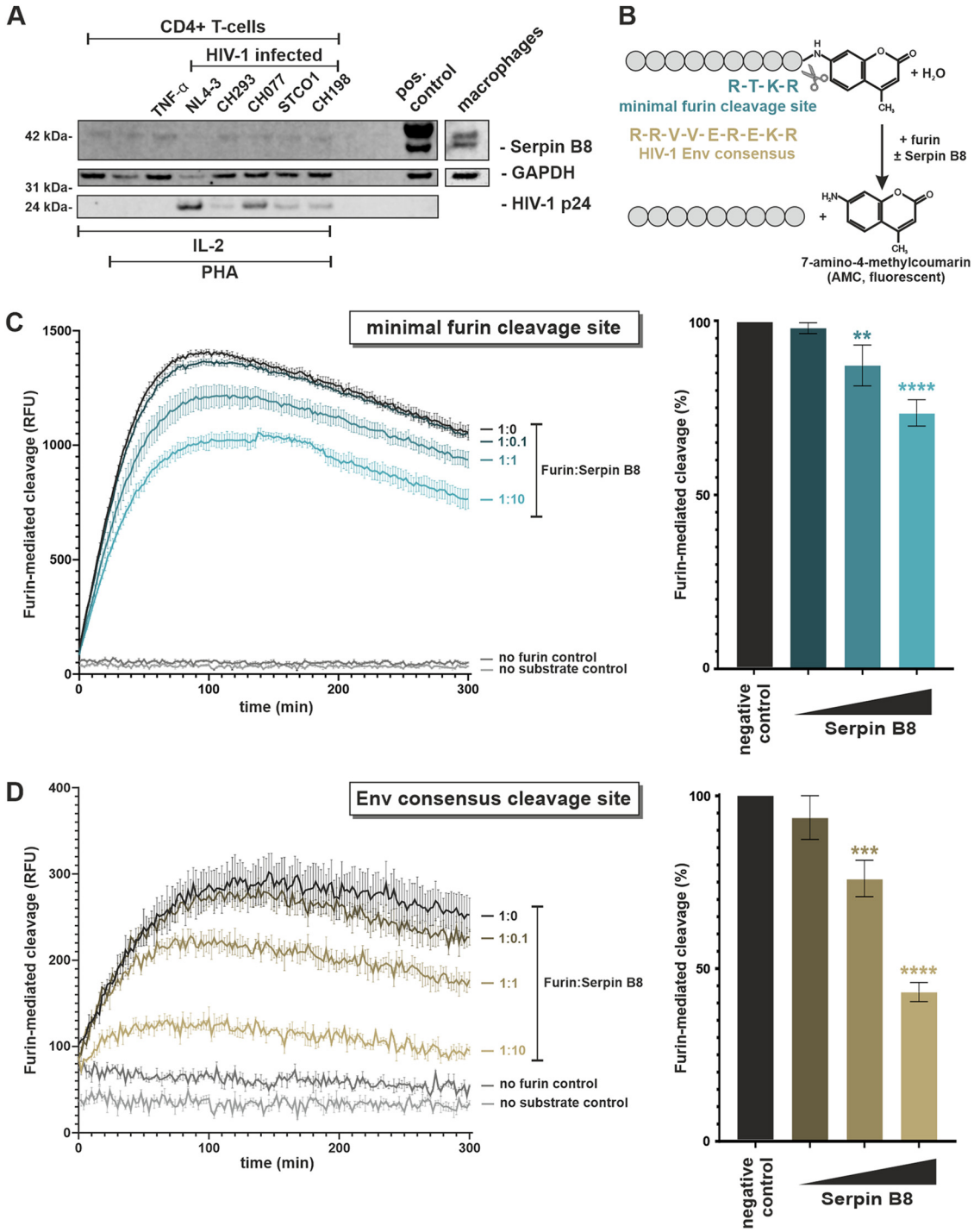

FIG 1 Serpin B8 is expressed in HIV-1 target cells and reduces furin activity *in vitro*. (A) Western blot of primary CD4$^+$ T cells and primary monocyte-derived macrophages. CD4$^+$ T cells were stimulated with IL-2, PHA or TNF-α as indicated, and infected with different clones of HIV-1 (NL4-3, CH293, CH077, STCO1, CH198). Three days postinfection, cells were lysed, and the amount of Serpin B8 was determined by Western blotting. A cell lysate of HEK293T cells overexpressing Serpin B8 served as positive control. Successful HIV-1 infection was validated via detection of HIV-1 capsid/p24; GAPDH served as loading control. (B) Principle of the furin activity assay: 7-amino-4-methylcoumarin (AMC)-based substrates harboring a minimal furin cleavage site (Arg-Thr-Lys-Arg) or the polybasic consensus cleavage site of HIV-1 Env (Arg-Arg-Val-Val-Glu-Arg-Glu-Lys-Arg) are converted into a fluorescent product by furin. (C, D) One nmol of reporter substrates harboring either (C) the minimal furin cleavage site or (D) the furin cleavage site of HIV-1 Env were coincubated with the indicated molar ratios of recombinant human furin and Serpin B8. Samples without substrate or without furin served as negative controls. Substrate conversion was monitored for 300 min as a reporter for furin activity. Representative experiments performed in technical triplicates (±SD) are shown on the left. The panels on the right show the mean areas under the curve (±SD) of three technical triplicates. ****, $P < 0.0001$; ***, $P < 0.001$; **, $P < 0.01$; *, $P < 0.05$.

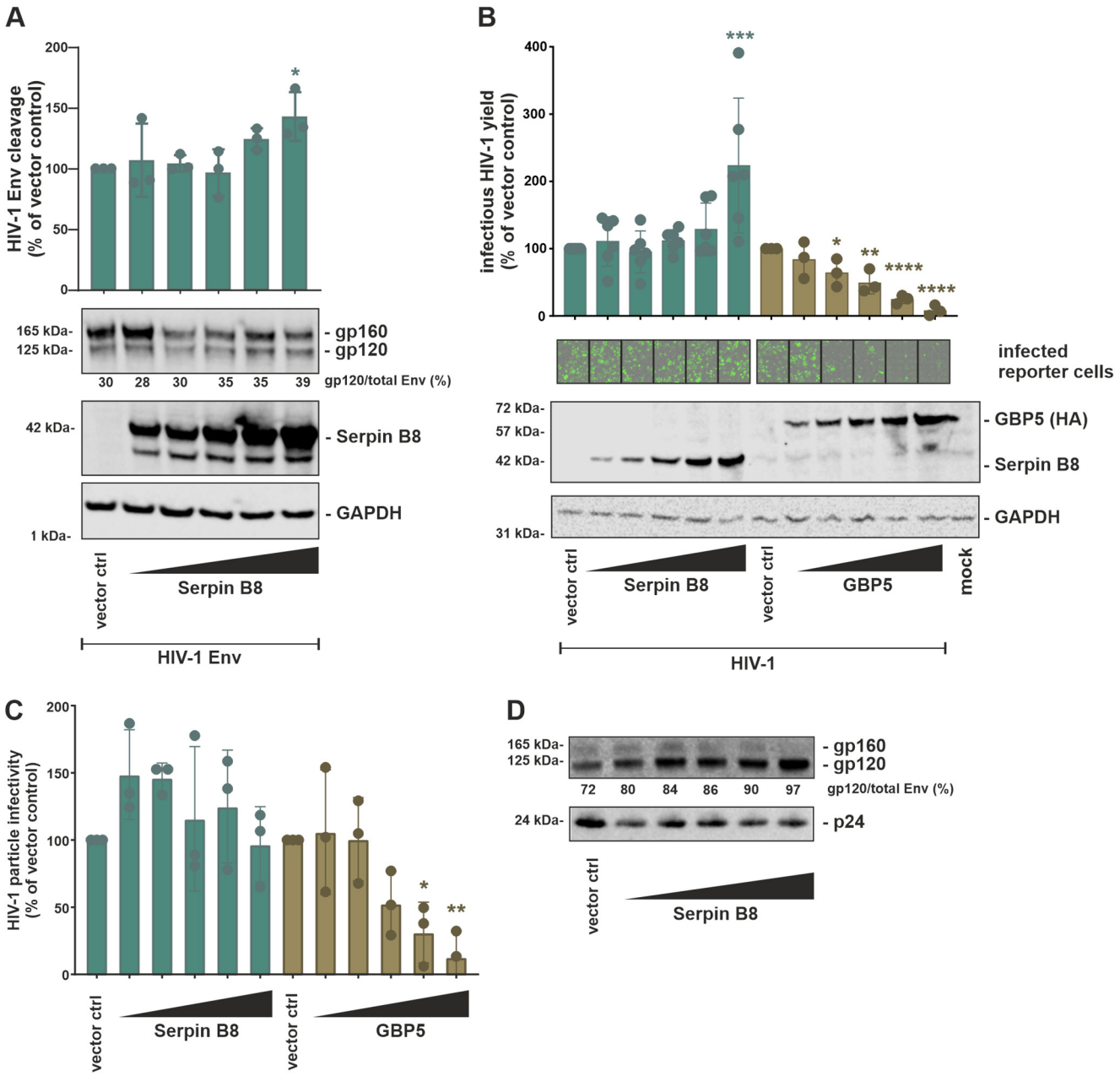

FIG 2 Serpin B8 does not reduce infectivity of newly produced HIV-1 particles. (A) HEK239T cells were cotransfected with expression plasmids for HIV-1 Env and Serpin B8. Two days posttransfection, cells were lysed and cleavage of the HIV-1 Env precursor gp160 into mature gp120 was monitored by Western blotting. GAPDH served as a loading control. One representative blot is shown at the bottom. Env cleavage was calculated by quantifying the percentage of gp120 to total Env (i.e., gp160 + gp120). Mean values of three independent experiments (±SD) are shown on top. (B) HEK293T cells were cotransfected with an infectious molecular clone of HIV-1 NL4-3 and expression plasmids for Serpin B8 or GBP5. Two days posttransfection, cells and supernatants were harvested. Western blotting was used to validate the expression of Serpin B8 and GBP5. One representative blot is shown at the bottom. Infectious HIV-1 yield was determined by infecting TZM-GFP reporter cells. GFP-expressing (i.e., HIV-1 infected) reporter cells of one representative experiment are shown in the middle panel. Mean infectious virus yields of three to six independent experiments (±SD) are shown on top. (C) The amount of HIV-1 p24/capsid protein in the supernatants of the experiment described in (B) were determined by ELISA. Relative virion infectivity was calculated by normalizing total infectious yield to the amount of p24. Mean values of three independent experiments (±SD) are shown. (D) Cleavage of immature HIV-1 Env gp160 into gp120 was monitored by Western blotting of the supernatants obtained from the experiment described in (B). The percentage of gp120 to total Env was calculated. One representative Western blot is shown. ****, $P < 0.0001$; ***, $P < 0.001$; **, $P < 0.01$; *, $P < 0.05$.

localization of Serpin B8 (13, 20–22). However, platelets have been shown to also release Serpin B8 upon their activation (11). In transfected HEK293T cells, immunofluorescence imaging showed no marked colocalization of furin with Serpin B8 (Fig. 3B). While furin was detected in juxtanuclear compartments and vesicular structures, Serpin B8 was evenly distributed throughout the cell. A similar distribution was observed in

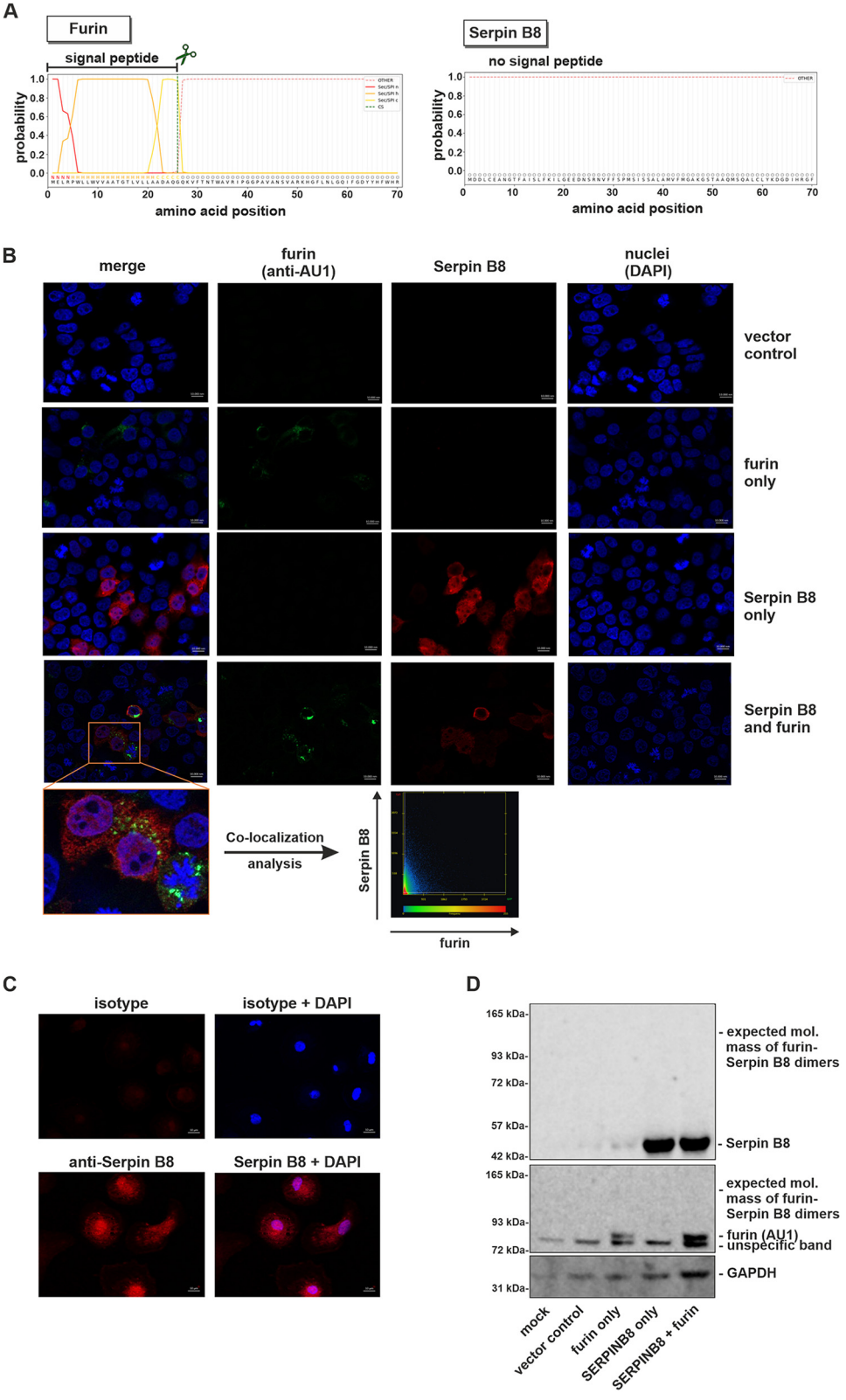

FIG 3 Serpin B8 does not colocalize with furin. (A) The presence and absence of a signal peptide in furin (top panel) or Serpin B8 (bottom panel), respectively, was predicted using SignalP-6.0 (44). Amino acid positions are indicated on the *x* axis. The signal peptide and its corresponding cleavage site are shown on top. (B) To monitor the subcellular localization of Serpin B8 and furin, HEK293T cells were cotransfected with expression plasmids for furin and/or Serpin B8. Two days posttransfection, cells were permeabilized, stained and analyzed

(Continued on next page)

primary monocyte-derived macrophages (Fig. 3C) and monocytes (13), suggesting that endogenous Serpin B8 does not enter the canonical secretory pathway in these cell types either. To further investigate whether Serpin B8 and furin interact with each other inside cells, we took advantage of the suicide mode-of-action of SERPINs that involves a covalent binding to their respective target proteases. In line with the lack of colocalization, however, covalent heterodimerization was not observed in HEK293T cells coexpressing Serpin B8 and furin (Fig. 3D). This strongly suggests that Serpin B8 fails to interfere with furin-mediated processing of HIV-1 Env as Serpin B8 and furin localize to different intracellular compartments.

Rerouting of Serpin B8 to the secretory pathway renders it active against HIV-1. Due to the lack of colocalization, we aimed at rendering Serpin B8 antivirally active by adding a signal peptide (SP) to its N terminus that relocalizes it to furin-containing compartments. We took advantage of the SP of PCSK5 (Fig. 4A), which has been shown to mediate entry of proteins into the secretory pathway (23). Successful relocalization was confirmed by immunofluorescence microscopy. While wild-type Serpin B8 was evenly distributed throughout the cytoplasm and the nucleus (Fig. 3B), Serpin B8 harboring a signal peptide (SP-Serpin B8) was localized to perinuclear and vesicular structures and colocalized with furin (Fig. 4B). Furthermore, the amount of proteolytically active furin in cell culture supernatants was reduced in the presence of SP-Serpin B8, but not wild type Serpin B8. (Fig. 4C and D). Most importantly, rerouted Serpin B8 also gained potent anti-HIV-1 activity and reduced infectious virus yield as efficiently as GBP5 (Fig. 4E and 2B). We also noted the appearance of a high-molecular weight band (105 to 110 kDa) suggesting that SP-Serpin B8 forms covalent dimers with a host protein (Fig. 4E). This band, however, was not detected by furin-specific antibodies. In line with inhibition of proteolytic Env activation, SP-Serpin B8 significantly reduced HIV-1 particle infectivity (Fig. 4F), decreased the ratio of mature to total Env in virus-producing cells and the amount of mature gp120 in newly produced virions (Fig. 4G).

Rerouted Serpin B8 reduces infectivity of pseudovirions carrying the glycoprotein GP of Marburg virus. Since several viral pathogens exploit furin for proteolytic maturation of their glycoproteins, we hypothesized that the antiviral activity of SP-Serpin B8 may not be limited to HIV-1. To test this hypothesis, we analyzed the effect of rerouted Serpin B8 on the infectivity of lentiviral pseudoparticles carrying the glycoprotein of Marburg virus. Marburg virus glycoprotein (GP) harbors a polybasic cleavage site (RRKR) that is cleaved by furin and/or related PCSKs (24). In a previous study (25), specific inhibition of furin reduced Marburg virus titers, but failed to completely block replication in Vero E6 cells. In line with our model that SP-Serpin B8 inhibits furin-mediated glycoprotein processing, SP-Serpin B8 dose-dependently reduced total infectious yield and relative infectivity of Marburg virus pseudovirions (Fig. 5A and B).

DISCUSSION

In our present study, we explored the ability of the cellular furin inhibitor Serpin B8 and a relocalized variant thereof to interfere with the maturation and infectivity of HIV-1 particles. We found that Serpin B8 has the potential to inhibit furin-mediated processing of the HIV-1 Env protein but requires rerouting to the secretory pathway to reduce infectious HIV-1 yield and particle infectivity.

The serine protease furin is exploited by a variety of viruses. These include enveloped viruses of the *retro-*, *herpes-*, *corona-*, *flavi-*, *toga-*, *borna-*, *bunya-*, *filo-*, *orthomyxo-*, *paramyxo-*, and *pneumoviridae*, whose envelope glycoproteins are activated by a proteolytic activation step, but also naked viruses such as papillomaviruses that use furin to prime

FIG 3 Legend (Continued)
by immunofluorescence microscopy (scale bar = 10 μm). A colocalization plot illustrating the signal intensities of furin and Serpin B8 for each pixel is shown at the bottom. (C) Primary monocyte-derived macrophages were stained for endogenous Serpin B8 (bottom) and analyzed via immunofluorescence microscopy (scale bar = 10 μm). An isotype control was used to determine unspecific background signals (top). (D) HEK293T cells were transfected with the indicated expression plasmids. Two days posttransfection, cells were lysed and analyzed by Western blotting. To detect Serpin B8, furin, and potential covalent heterodimers thereof, the membrane was probed with antibodies against Serpin B8 (top) and the AU1 tag of furin (middle). GAPDH served as loading control (bottom).

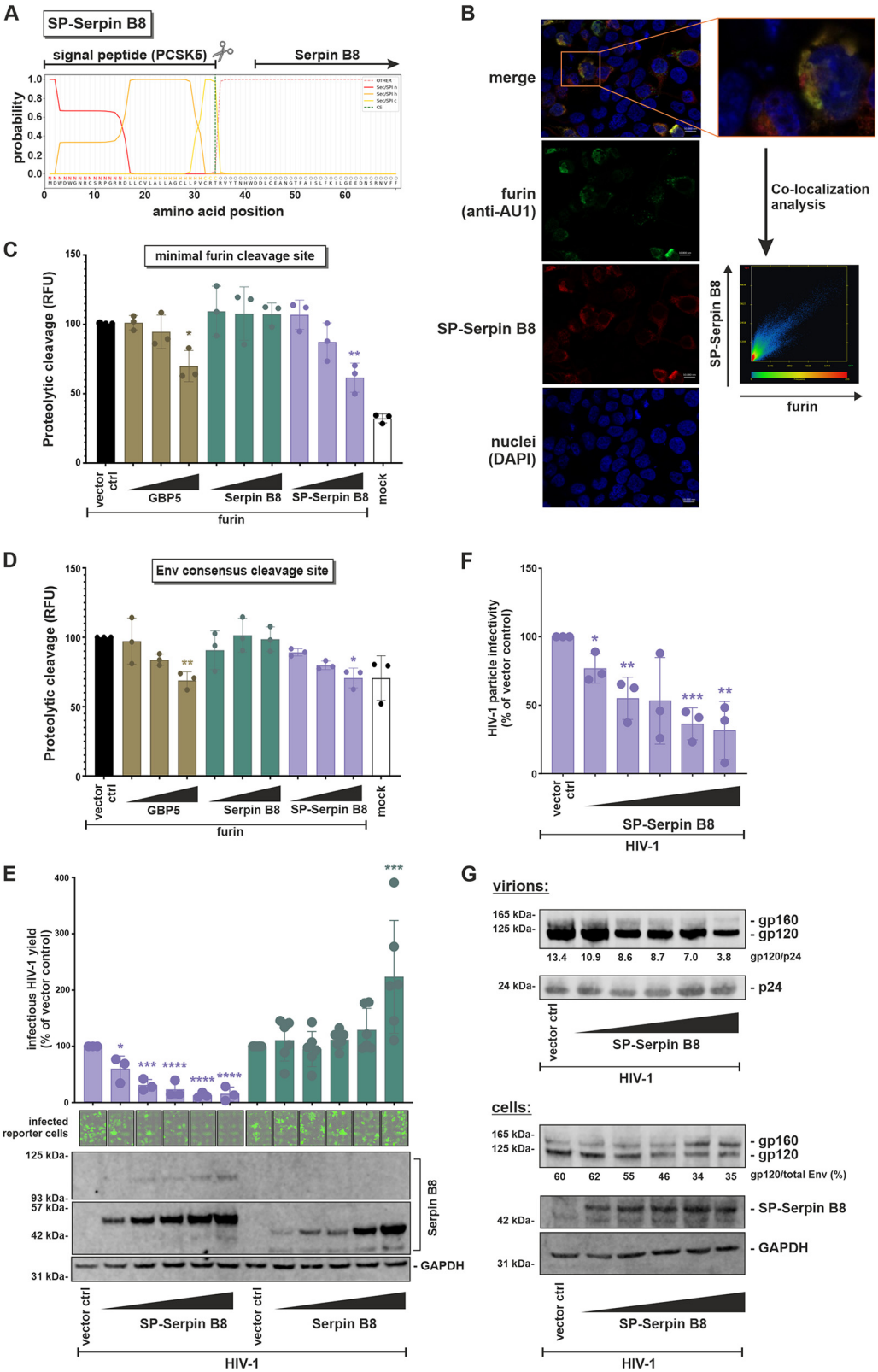

FIG 4 Rerouting of Serpin B8 to the secretory pathway renders it active against HIV-1. (A) Fusion of the signal peptide of murine PCSK5 to the N terminus of human Serpin B8. The presence of a signal peptide was predicted using SignalP-6.0 (44). (B) Immunofluorescence microscopy of HEK239T cells cotransfected with expression plasmids for furin and Serpin B8 harboring an N-terminal signal peptide (SP-Serpin B8). A colocalization plot is shown on the right. (C, D) To analyze the effect of SP-Serpin B8 on furin activity, supernatants of HEK293T cells cotransfected with expression plasmids for furin

(Continued on next page)

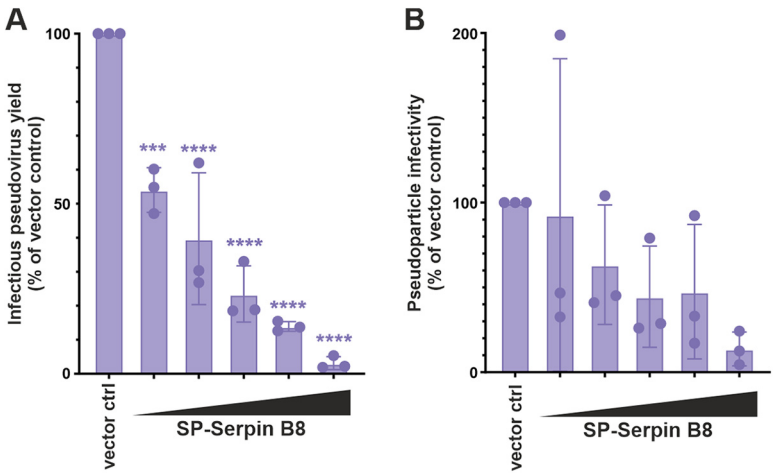

FIG 5 Rerouted Serpin B8 reduces infectivity of pseudovirions carrying the glycoprotein of Marburg virus. (A, B) Lentiviral luciferase reporter viruses carrying the glycoprotein of Marburg virus were generated in the presence of increasing amounts of SP-Serpin B8. (A) Total infectious pseudovirus yield was determined by infecting HEK293T cells and subsequent quantification of luciferase activity. (B) Relative pseudovirion infectivity was determined by normalizing total infectivity to the amount of p24 as determined by ELISA. Mean values of three independent experiments (±SD) are shown. ****, $P < 0.0001$; ***, $P < 0.001$.

their capsid proteins (1). This broad dependency of viruses on furin may be the consequence of the expression of this protease in essentially all cell types and tissues (1). Since furin enters the secretory pathway, it can activate viral proteins not only in infected producer cells, but also the extracellular space or upon viral entry into new target cells (1).

Intriguingly, host factors inhibiting the enzymatic activity of furin and other host proteases have emerged as components of the immune response against viruses as they reduce virion infectivity by suppressing viral protein maturation. For example, the G-protein coupled receptor PAR1 traps furin in the trans-Golgi network and inhibits its ability to process HIV-1 Env (26, 27). Similarly, the IFN-inducible proteins GBP2 and GBP5 reduce furin activity, thereby inhibiting the spread of HIV-1, measles, Zika, SARS-CoV-2, and other furin-dependent viruses (17, 28). We therefore hypothesized that another endogenous furin inhibitor, Serpin B8, may also negatively interfere with the replication of HIV-1 and potentially other viral pathogens.

In contrast to other Serpins, Serpin B8 lacks an N-terminal signal peptide (Fig. 3A), suggesting that it is not released via the canonical secretory pathway. Dahlen and colleagues hypothesized that two hydrophobic regions (H1 and H2) at its N terminus might mediate its release (29). Similar secretion motifs have been reported for Serpin B14 (=Ovalbumin) (30) and Serpin B2 (=PAI-2) (31). In line with a noncanonical mode of release, Serpin B8 was evenly distributed throughout the cytoplasm and the nucleus of primary macrophages (Fig. 3C) and transfected HEK293T cells and did not colocalize

FIG 4 Legend (Continued)
and increasing amounts of the indicated Serpin B8 variants were harvested 2 days posttransfection. The proteolytic activity in the culture supernatants was analyzed using the AMC reporter assay described in Fig. 1B. Mean values of three independent experiments (±SD) are shown. (E) HEK293T cells were cotransfected with an infectious molecular clone of HIV-1 NL4-3 and expression plasmids for the indicated Serpin B8 variants. Two days posttransfection, cells and supernatants were harvested. Western blotting was used to validate expression of Serpin B8. One representative blot is shown at the bottom. Two days posttransfection, infectious HIV-1 yield was determined by infecting TZM-GFP reporter cells. GFP-expressing (i.e., HIV-1 infected) reporter cells of one representative experiment are shown in the middle panel. Mean infectious virus yields of three to six independent experiments (±SD) are shown on top. (F) Relative virion infectivity was calculated by normalizing total infectious yield to the amount of p24 as determined by ELISA. Mean values of three independent experiments (±SD) are shown. (G) Western blotting was performed to determine Env levels in virions (top) and cell lysates (bottom) of the experiment described in panel E. GAPDH served as a loading control for cell lysates, while p24 was detected to monitor the amount of viral capsid protein in the supernatants. One representative blot is shown for virions and cells, respectively. ****, $P < 0.0001$; ***, $P < 0.001$; **, $P < 0.01$; *, $P < 0.05$.

with furin in the secretory pathway (Fig. 3B). This intracellular lack of interaction also explains why overexpression of Serpin B8 did not reduce furin-mediated Env maturation or infectious HIV-1 production. Even if the two proteins do not colocalize within cells, Serpin B8 may inhibit furin in the extracellular space. Yet, this inhibition comes too late to exert any antiretroviral effect, since HIV-1 Env has already been proteolytically activated during its transport to the cell surface. It is therefore unlikely that Serpin B8 reduces HIV-1 Env maturation and thus virion infectivity *in vivo*. The same is true for Marburg virus, whose glycoprotein is also cleaved in producer cells (24). In contrast, viral proteins that are proteolytically processed after virion release may be susceptible to Serpin B8. Two examples are the prM protein of Dengue virus (32) and the minor capsid protein L2 of human papillomaviruses (33). Thus, Serpin B8 may still restrict some furin-dependent viruses, even though it fails to inhibit HIV-1 Env maturation.

Surprisingly, overexpression of Serpin B8 even modestly enhanced the processing of immature HIV-1 gp160 into its mature forms and increased infectivity of newly produced virions. The molecular mechanism underlying this enhancing effect remains enigmatic. It is tempting to speculate that Serpin B8 inhibits a protease other than furin that exerts direct or indirect antiviral effects. Besides furin (29), Serpin B8 blocks the proteolytic activity of trypsin, thrombin, Factor Xa, subtilisin A (10), and chymotrypsin (29). However, the *in vivo* relevance of these findings remains unclear since these targets were identified using *in vitro* assays and include nonhuman proteases. Intriguingly, two independent loss-of-function mutations in Serpin B8 were identified in families suffering from an autosomal-recessive form of exfoliative ichthyosis (34). Thus, Serpin B8 seems to exert an important physiological role in maintaining mechanical stability of the skin. In agreement with this, Serpin B8 is readily detected in squamous epithelia (13), and siRNA-mediated depletion of Serpin B8 results in a cell-cell adhesion defect (34). It is therefore tempting to speculate that Serpin B8 targets a protease that plays an important role in skin development and/or integrity.

Most importantly, the addition of an N-terminal signal peptide to Serpin B8 turned Serpin B8 into a potent inhibitor of HIV-1. While wild type (wt) Serpin B8 slightly enhanced infectious HIV-1 production (Fig. 2B), the rerouted variant reduced virion infectivity by more than 50% (Fig. 4F) and total infectious HIV-1 yield by more than 80% (Fig. 4E). Furthermore, SP-Serpin B8 reduced infectivity of lentiviruses carrying the glycoprotein of Marburg virus, which is also cleaved by furin and/or related PCSKs (24).

In cells expressing the Serpin B8 variant with signal peptide, we also detected a 105- to 110-kDa protein by Western blotting using a Serpin B8-specific antibody (Fig. 4E). A similar high-molecular-weight band was absent from cells overexpressing wild-type Serpin B8. We initially hypothesized that this band represents a covalent heterodimer of SP-Serpin B8 with furin. However, a dimer of Serpin B8 (~43 kDa after removal of the SP) and mature furin (90 to 98 kDa) is expected to show a higher apparent molecular weight. Furthermore, the 105- to 110-kDa protein could not be detected using a furin-specific antibody (data not shown). Thus, Serpin B8 may target yet another protease in the secretory pathway of HEK293T cells. This is not surprising given its broad inhibitory activity *in vitro*, including the inhibition of bacterial subtilisin A (10). Nevertheless, inhibition of furin by SP-Serpin B8 could be validated since overexpression of furin increased cleavage of polybasic 7-amino-4-methylcoumarin (AMC) substrates in the presence of wild-type Serpin B8, but not SP-Serpin B8.

While the full protease target spectrum of Serpin B8 remains to be elucidated, our results provide important insights into the biology of Serpin B8 and help to understand its role in inhibiting proteases involved in viral replication. Moreover, a direct comparison of Serpin B8 variants that are released via the canonical (SP-Serpin B8) or noncanonical (wild type) secretory pathway may serve as useful tool to determine the exact site and timing of viral or host protein processing. Finally, we here present an example of protein engineering that confers antiviral activity to a host protein by rerouting it and may help to advance therapeutic approaches that aim at targeting furin or other host proteases to inhibit viral spread.

MATERIALS AND METHODS

Cell culture. HEK293T cells were cultured in DMEM containing 10% heat-inactivated fetal calf serum (FCS) plus 2 mM L-glutamine, 100 μg/mL streptomycin and 100 units/mL penicillin and were cultured at 37°C, 90% humidity, and 5% CO_2. They were provided and authenticated by the ATCC. HEK293T cells were isolated from a female fetus and first described by DuBridge et al. (35). TZM-GFP cells were obtained through the NIH HIV Reagent Program, NIAID, NIH and contributed by David G. Russell and David W. Gludish (18). TZM-GFP cells are derived from HeLa cells, which were isolated from a 30-year-old female. They express the HIV-1 entry receptors (CD4, CXCR4, CCR5). GFP is expressed under the control of the HIV-1 long terminal repeat (LTR) promoter and serves as a reporter for HIV-1 infection.

Isolation of primary cells. Peripheral blood mononuclear cells (PBMCs) from healthy human donors were isolated using lymphocyte separation medium. $CD4^+$ T cells were negatively isolated using the RosetteSep human $CD4^+$ T cell enrichment cocktail (StemCell) according to the manufacturer's instructions. $CD4^+$ T cells were cultured in RPMI 1640 medium supplemented with FCS (10%), glutamine (2 mM), streptomycin (100 mg/mL), penicillin (100 U/mL), and interleukin-2 (IL-2) (10 ng/mL) at 37°C, 90% humidity, and 5% CO_2.

Macrophages were generated from buffy coats essentially as described (36). Briefly, PBMCs were isolated from buffy coats by Ficoll-Paque PLUS density gradient centrifugation and 2×10^7 PBMCs were seeded in petri dishes in RPMI medium supplemented with 4% human AB serum, 2 mM L-glutamine, 100 μg/mL penicillin-streptomycin, 1 mM sodium pyruvate, 1× nonessential amino acids and 0.4× MEM vitamins. Monocytes were differentiated for 3 days by plastic adherence into monocyte-derived macrophages (MDM). After 3 days, nonadherent cells were removed by washing and the MDM were further differentiated for 4 days. Accutase was used to detach the MDM for 45 min at 37°C. The cells were then directly processed for Western blot. The use of PBMCs from healthy human donors was approved by the local ethics committee (507/2017B01 and 127/2022BO2).

Expression plasmids and proviral constructs. C-terminally AU1-tagged human furin (17) and N-terminally HA-tagged human GBP5 (37) were expressed from pCG-based expression vectors that have been described before. Both genes had been inserted via XbaI and MluI. The furin expression plasmid coexpresses blue fluorescent protein (BFP) via an IRES. A pCG construct harboring HIV-1 NL4-3 *nef* with premature stop codons, which expresses eGFP, was used as empty vector control (38). HIV-1 NL4-3 Env (untagged) was inserted into pCAGGS via EcoRI and KpnI essentially as described before. Infectious molecular clones of HIV-1 NL4-3 92TH014-12 (39), CH293 (40), CH077 (41), STCO1 (40), and CH198 (40) have been described before. The HIV-1 NL4-3 clone was obtained via the National Institutes of Health (cat. no. 114). The HIV-1 NL4-3 *env* stop firefly luciferase reporter plasmid and pCAGGS expression plasmid for Marburg virus glycoprotein that were used for pseudotyping have been described before (17, 42, 43). C-terminally myc-tagged human Serpin B8 was expressed from a CMV-promoter based plasmid (pCMV6) purchased from OriGene Technologies (cat. no. RC223880). The nucleotides encoding the signal peptide of murine PCSK5 (nt 1 to 123) were added to the 5′ end of Serpin B8 via overlap extension PCR. The resulting fusion construct was inserted into pCMV6 via BglII and MluI.

Transfection. HEK293T cells were transiently transfected using the calcium-phosphate precipitation method. One day before transfection, 6×10^5 HEK293T cells were seeded in 6-well plates in 2 mL supplemented DMEM to obtain a confluence of 50% to 60% at the time of transfection. For transfection, 5 μg DNA was mixed with 13 μL 2 M $CaCl_2$ and filled up with water to 100 μL. Afterwards, 100 μL 2× 4-(2-hydroxyethyl)-1-piperazineethanesulfonic acid buffered saline (HBS) was added, mixed, and added dropwise to the cells. Medium change was performed 16 h after transfection.

Stimulation and infection of $CD4^+$ T cells. Isolated $CD4^+$ T cells were stimulated with 1 μg/mL IL-2 and 1 μg/mL phytohemagglutinin (PHA). An additional control was costimulated with 100 ng/mL of TNF-α. Two days later, 1×10^6 stimulated cells were infected by spinoculation with 1:1.2 diluted supernatant of HEK293T, transfected with different HIV-1 plasmids. Spinoculation was performed at 1,200 rcf for 120 min at 37°C. Afterwards, the cells were incubated in RPMI media with 1 μg/mL IL-2 at 37°C, 90% humidity, and 5% CO_2. Three days later, the cells were processed for Western blot.

Gel electrophoresis and Western blot. Two days after transfection, cells were washed in PBS and subsequently lysed in Western blot lysis buffer (150 mM NaCl, 50 mM HEPES, 5 mM EDTA, 0.1% NP-40, 500 mM Na_3VO_4, 500 mM NaF, pH 7.5) supplemented with a protease inhibitor pill (Roche, no. 5892791001). After incubating on ice for 20 min, the samples were centrifuged (4°C, 20 min, 20,817 × *g*) and the supernatant was transferred to a fresh tube for further analysis. Whole-cell lysates were mixed with protein sample loading buffer (LI-COR) supplemented with 10% β-mercaptoethanol (Sigma-Aldrich), heated at 95°C for 5 min, separated on NuPAGE 4 to 12% Bis-Tris gels (Invitrogen) for 80 min at 120 V and blotted onto Immobilon-FL PVDF membranes (Merck Millipore). The transfer was performed at a constant voltage of 30 V for 30 min. After transfer, the membrane was blocked in 5% milk in PBS (Thermo Scientific). Proteins were stained using primary antibodies against Serpin B8 (santa cruz, no. 101371), GAPDH (Biolegend, no. 607902); HIV-1 Env (NIH, no. 12559); HA-tag (abcam, no. 18181), HIV-1 p24 (abcam, no. 9071) and infrared dye labeled secondary antibodies (LI-COR IRDye). Membranes were scanned using LI-COR and band intensities were quantified using Image Studio Lite version 5.2. (LI-COR).

To process supernatants for Western blotting, 200 μL of 20% sucrose (Sigma-Aldrich) were overlaid with 1,000 μL supernatant and then centrifuged (4°C, 90 min, 20,817 × *g*). Afterwards, the supernatant was taken off, and the remaining virus pellet was resuspended in 10 μL lysis buffer supplemented with protein sample loading buffer and β-mercaptoethanol.

AMC reporter assays. In a 96-well format, 100 ng (RTKR-substrate) or 200 ng (Env substrate) of recombinant human furin (BioLegend, no. 719402) was incubated with different amounts of recombinant human Serpin B8 (Biorbyt Ltd., no. 754692) (1:10, 1:1, 10:1) for 30 min at room temperature (RT). Afterwards, 1 nmol of a 7-amino-4-methylcoumarin (AMC) substrate harboring the minimal target

sequence for furin or the consensus cleavage site of Env (Nanjing Biotech) was added per well with a final volume of 100 μL and a final concentration of 1 mM $CaCl_2$ in water. Furin-mediated cleavage was determined every 2 min for 5 h, using a Cytation 3 Imaging Reader (355 nm excitation and 460 nm emission).

To determine the proteolytic activity in cell culture supernatants, HEK293T cells were cotransfected with expression plasmids for furin and GBP5 or SERPINB8 (wild type or with signal peptide) in different ratios (1:4, 1:1, 4:1). Two days posttransfection, supernatants were harvested. The activity assay was performed using 20 μL of supernatant and 1 nmol AMC substrate (RTKR and Env). Proteolytic cleavage was determined every 3 min for 5 h, using a Cytation 3 imaging reader (355 nm excitation and 460 nm emission).

ELISA. To determine the amounts of HIV-1 virions present in the supernatants of infected cells, the p24 capsid protein was quantified using a home-made p24 sandwich ELISA. High-binding ELISA plates (Sarstedt, no. 82.1581.200) were coated with the p24-coating antibody (ExBio, no. 11-CM006-BULK) overnight at RT. Plates were washed, blocked with PBS supplemented with 10% FCS for 1 h at 37°C and washed again before adding samples and p24 protein standard. After overnight incubation, plates were washed, incubated with a polyclonal anti-HIV p24 antiserum (Eurogentech, produced on demand) and a secondary HRP-conjugated antibody (Dianova, no. 111-035-008), each for 1 h at 37°C. Plates were washed again, 3,3′,5,5′-Tetramethylbenzidine (TMB) substrate was added and after several minutes of incubation the reaction was stopped with 0.5 M H_2SO_4. Absorption was measured at 450 nm with a baseline correction at 650 nm using a microplate reader.

TZM-GFP reporter assay. To determine infectious HIV-1 yield, 6,000 TZM-GFP cells per well were seeded in a 96-well plate and infected with different dilutions of cell culture supernatant in triplicates on the following day. Three days postinfection, GFP expression was quantified using an Incucyte imaging device. The area of GFP positive cells was normalized to the total area of cells.

Pseudotyping assay. For pseudotyping, HEK293T cells were cotransfected with an HIV-1 NL4-3 *env* stop firefly luciferase reporter plasmid and an expression plasmid for the viral glycoprotein of Marburg virus (DNA ratio of HIV-1 NL4-3 *env* stop/viral glycoprotein: 1.225 μg/0.025 μg [17] in a 12-well format). Virus stocks were used to transduce HEK293T cells in triplicates, which were seeded 1 day prior to transduction in a 96-well plate format in a density of 10,000 cells/well. Three days postransduction, firefly luciferase activity was measured using luciferase cell culture lysis 5× reagent and luciferase assay system (Promega) according to the manufacturer's instructions.

Immunofluorescence microscopy. 1.5×10^5 HEK293T cells in 500 μL DMEM were seeded on coverslips coated with poly-L-lysine (PLL) in a 24-well plate. On the following day, cells were transfected using Lipofectamine 2000 (Invitrogen, no. 11668019) following the manufacturer's instructions (800 ng DNA, 1.5 μL lipofectamine, 50 μL Opti-MEM). Staining was performed one or two days posttransfection. First, the cells were washed once with cold PBS and fixed with 4% PFA in PBS for 20 min at room temperature. After washing with PBS, the cells were stained with primary antibodies against Serpin B8 (Santa Cruz, no. 101371, 4 μg/mL) and AU1 tag (Novus Biologicals, no. NB600-453, 4 μg/mL) (1.5 h each) and secondary antibodies donkey antimouse AF555 and donkey antirabbit AF488 (1 h). For DNA staining, DAPI (200 ng/mL) was applied for 30 s. After washing, the coverslips were mounted in 10 μL Mowiol mounting medium (Carl Roth) and sealed using nail polish. Macrophages were seeded on coverslips in a 24-well format at a density of 1×10^6 cells/well. One day later, cells were fixed, washed, and stained for Serpin B8 and DAPI as outlined above. Confocal microscopy was performed using an LSM710 (Carl Zeiss).

Signal peptide prediction. The presence or absence of an N-terminal signal peptide was predicted using SignalP-6.0 using the following settings: Organism: Eukarya; Output format: Long output; Model mode: Slow (44).

Statistical analyses. All statistical calculations were performed using GraphPad PRISM 8. *P* values were determined using one-way ANOVA. Unless otherwise stated, data are shown as the mean of at least three independent experiments ± SD.

ACKNOWLEDGMENTS

We thank Corinna Bay for excellent technical assistance and the Interdisciplinary Doctoral Program in Medicine of the University Hospital Tübingen for training and support. We also thank Fabian Zech for helpful advice and protocols. M.P. was funded by the Interdisciplinary Doctoral Program in Medicine of the University Hospital Tübingen and the German Center for Infection Research (DZIF, TI 07.003_Petersen). D.S. was supported by SPP1923 and the Heisenberg Program of the German Research Foundation (SA 2676/3-1; SA 2676/1-2), as well as the Canon Foundation Europe. K.H. is supported by the fortüne program of the Medical Faculty of the University of Tübingen. T.B. was funded by the Nazarbayev University Faculty-Development Competitive Research Grants Program, reference: 20122022FD4123. The funders had no role in study design, data collection and interpretation, or the decision to submit the work for publication.

REFERENCES

1. Braun E, Sauter D. 2019. Furin-mediated protein processing in infectious diseases and cancer. Clin Transl Immunology 8:e1073. https://doi.org/10.1002/cti2.1073.
2. Law RH, Zhang Q, McGowan S, Buckle AM, Silverman GA, Wong W, Rosado CJ, Langendorf CG, Pike RN, Bird PI, Whisstock JC. 2006. An overview of the serpin superfamily. Genome Biol 7:216. https://doi.org/10.1186/gb-2006-7-5-216.

3. Dittmann M, Hoffmann HH, Scull MA, Gilmore RH, Bell KL, Ciancanelli M, Wilson SJ, Crotta S, Yu Y, Flatley B, Xiao JW, Casanova JL, Wack A, Bieniasz PD, Rice CM. 2015. A serpin shapes the extracellular environment to prevent influenza A virus maturation. Cell 160:631–643. https://doi.org/10.1016/j.cell.2015.01.040.
4. Azouz NP, Klingler AM, Callahan V, Akhrymuk IV, Elez K, Raich L, Henry BM, Benoit JL, Benoit SW, Noe F, Kehn-Hall K, Rothenberg ME. 2021. Alpha 1 antitrypsin is an inhibitor of the SARS-CoV-2-priming protease TMPRSS2. Pathog Immun 6:55–74. https://doi.org/10.20411/pai.v6i1.408.
5. Rosendal E, Mihai IS, Becker M, Das D, Frangsmyr L, Persson BD, Rankin GD, Groning R, Trygg J, Forsell M, Ankarklev J, Blomberg A, Henriksson J, Overby AK, Lenman A. 2022. Serine protease inhibitors restrict host susceptibility to SARS-CoV-2 infections. mBio 13:e0089222. https://doi.org/10.1128/mbio.00892-22.
6. Wettstein L, Immenschuh P, Weil T, Conzelmann C, Almeida-Hernandez Y, Hoffmann M, Kempf A, Nehlmeier I, Lotke R, Petersen M, Stenger S, Kirchhoff F, Sauter D, Pohlmann S, Sanchez-Garcia E, Munch J. 2023. Native and activated antithrombin inhibits TMPRSS2 activity and SARS-CoV-2 infection. J Med Virol 95:e28124. https://doi.org/10.1002/jmv.28124.
7. Singh S, O'Reilly S, Gewaid H, Bowie AG, Gautier V, Worrall DM. 2022. Reactive centre loop mutagenesis of SerpinB3 to target TMPRSS2 and furin: inhibition of SARS-CoV-2 cell entry and replication. Int J Mol Sci 23.
8. Banno T, Gazel A, Blumenberg M. 2004. Effects of tumor necrosis factor-alpha (TNF alpha) in epidermal keratinocytes revealed using global transcriptional profiling. J Biol Chem 279:32633–32642. https://doi.org/10.1074/jbc.M400642200.
9. Ah-Kim H, Zhang X, Islam S, Sofi JI, Glickberg Y, Malemud CJ, Moskowitz RW, Haqqi TM. 2000. Tumour necrosis factor alpha enhances the expression of hydroxyl lyase, cytoplasmic antiproteinase-2 and a dual specificity kinase TTK in human chondrocyte-like cells. Cytokine 12:142–150. https://doi.org/10.1006/cyto.1999.0539.
10. Dahlen JR, Foster DC, Kisiel W. 1997. Expression, Purification, and Inhibitory Properties of Human Proteinase Inhibitor 8. Biochemistry 36:14874–14882. https://doi.org/10.1021/bi970977p.
11. Leblond J, Laprise MH, Gaudreau S, Grondin F, Kisiel W, Dubois CM. 2006. The serpin proteinase inhibitor 8: an endogenous furin inhibitor released from human platelets. Thromb Haemost 95:243–252. https://doi.org/10.1160/TH05-08-0561.
12. Uhlen M, Fagerberg L, Hallstrom BM, Lindskog C, Oksvold P, Mardinoglu A, Sivertsson A, Kampf C, Sjostedt E, Asplund A, Olsson I, Edlund K, Lundberg E, Navani S, Szigyarto CA, Odeberg J, Djureinovic D, Takanen JO, Hober S, Alm T, Edqvist PH, Berling H, Tegel H, Mulder J, Rockberg J, Nilsson P, Schwenk JM, Hamsten M, von Feilitzen K, Forsberg M, Persson L, Johansson F, Zwahlen M, von Heijne G, Nielsen J, Ponten F. 2015. Proteomics. Tissue-based map of the human proteome. Science 347:1260419. https://doi.org/10.1126/science.1260419.
13. Strik MC, Bladergroen BA, Wouters D, Kisiel W, Hooijberg JH, Verlaan AR, Hordijk PL, Schneider P, Hack CE, Kummer JA. 2002. Distribution of the human intracellular serpin protease inhibitor 8 in human tissues. J Histochem Cytochem 50:1443–1454. https://doi.org/10.1177/002215540205001103.
14. Seidah NG, Prat A. 2012. The biology and therapeutic targeting of the proprotein convertases. Nat Rev Drug Discov 11:367–383. https://doi.org/10.1038/nrd3699.
15. Lamango NS, Zhu X, Lindberg I. 1996. Purification and enzymatic characterization of recombinant prohormone convertase 2: stabilization of activity by 21 kDa 7B2. Arch Biochem Biophys 330:238–250. https://doi.org/10.1006/abbi.1996.0249.
16. Rezaie AR. 1998. Calcium enhances heparin catalysis of the antithrombin-factor Xa reaction by a template mechanism. Evidence that calcium alleviates Gla domain antagonism of heparin binding to factor Xa. J Biol Chem 273:16824–16827. https://doi.org/10.1074/jbc.273.27.16824.
17. Braun E, Hotter D, Koepke L, Zech F, Groß R, Sparrer KMJ, Müller JA, Pfaller CK, Heusinger E, Wombacher R, Sutter K, Dittmer U, Winkler M, Simmons G, Jakobsen MR, Conzelmann K-K, Pöhlmann S, Münch J, Fackler OT, Kirchhoff F, Sauter D. 2019. Guanylate-binding proteins 2 and 5 exert broad antiviral activity by inhibiting furin-mediated processing of viral envelope proteins. Cell Rep 27:2092–2104.e10. https://doi.org/10.1016/j.celrep.2019.04.063.
18. Gludish DW, Boliar S, Caldwell S, Tembo DL, Chimbayo ET, Jambo KC, Mwandumba HC, Russell DG. 2020. TZM-gfp cells: a tractable fluorescent tool for analysis of rare and early HIV-1 infection. Sci Rep 10:19900. https://doi.org/10.1038/s41598-020-76422-6.
19. Bartuski AJ, Kamachi Y, Schick C, Overhauser J, Silverman GA. 1997. Cytoplasmic antiproteinase 2 (PI8) and bomapin (PI10) map to the serpin cluster at 18q21.3. Genomics 43:321–328. https://doi.org/10.1006/geno.1997.4827.
20. Gillard A, Scarff K, Loveland KL, Ricardo SD, Bird PI. 2006. Modulation and redistribution of proteinase inhibitor 8 (Serpinb8) during kidney regeneration. Am J Nephrol 26:34–42. https://doi.org/10.1159/000091784.
21. Sprecher CA, Morgenstern KA, Mathewes S, Dahlen JR, Schrader SK, Foster DC, Kisiel W. 1995. Molecular cloning, expression, and partial characterization of two novel members of the ovalbumin family of serine proteinase inhibitors. J Biol Chem 270:29854–29861. https://doi.org/10.1074/jbc.270.50.29854.
22. Bird CH, Blink EJ, Hirst CE, Buzza MS, Steele PM, Sun J, Jans DA, Bird PI. 2001. Nucleocytoplasmic distribution of the ovalbumin serpin PI-9 requires a nonconventional nuclear import pathway and the export factor Crm1. Mol Cell Biol 21:5396–5407. https://doi.org/10.1128/MCB.21.16.5396-5407.2001.
23. Zhu J, Declercq J, Roucourt B, Ghassabeh GH, Meulemans S, Kinne J, David G, Vermorken AJ, Van de Ven WJ, Lindberg I, Muyldermans S, Creemers JW. 2012. Generation and characterization of non-competitive furin-inhibiting nanobodies. Biochem J 448:73–82. https://doi.org/10.1042/BJ20120537.
24. Volchkov VE, Volchkova VA, Stroher U, Becker S, Dolnik O, Cieplik M, Garten W, Klenk HD, Feldmann H. 2000. Proteolytic processing of Marburg virus glycoprotein. Virology 268:1–6. https://doi.org/10.1006/viro.1999.0110.
25. Stroher U, Willihnganz L, Jean F, Feldmann H. 2007. Blockage of filoviral glycoprotein processing by use of a protein-based inhibitor. J Infect Dis 196 Suppl 2:S271–5. https://doi.org/10.1086/520592.
26. Kim W, Zekas E, Lodge R, Susan-Resiga D, Marcinkiewicz E, Essalmani R, Mihara K, Ramachandran R, Asahchop E, Gelman B, Cohen EA, Power C, Hollenberg MD, Seidah NG. 2015. Neuroinflammation-induced interactions between protease-activated receptor 1 and proprotein convertases in hiv-associated neurocognitive disorder. Mol Cell Biol 35:3684–3700. https://doi.org/10.1128/MCB.00764-15.
27. Sachan V, Lodge R, Mihara K, Hamelin J, Power C, Gelman BB, Hollenberg MD, Cohen EA, Seidah NG. 2019. HIV-induced neuroinflammation: impact of PAR1 and PAR2 processing by Furin. Cell Death Differ 26:1942–1954. https://doi.org/10.1038/s41418-018-0264-7.
28. Mesner D, Reuschl AK, Whelan MVX, Bronzovich T, Haider T, Thorne LG, Ragazzini R, Bonfanti P, Towers GJ, Jolly C. 2023. SARS-CoV-2 evolution influences GBP and IFITM sensitivity. Proc Natl Acad Sci U S A 120:e2212577120. https://doi.org/10.1073/pnas.2212577120.
29. Dahlen JR, Jean F, Thomas G, Foster DC, Kisiel W. 1998. Inhibition of soluble recombinant furin by human proteinase inhibitor 8. J Biol Chem 273:1851–1854. https://doi.org/10.1074/jbc.273.4.1851.
30. Tabe L, Krieg P, Strachan R, Jackson D, Wallis E, Colman A. 1984. Segregation of mutant ovalbumins and ovalbumin-globin fusion proteins in Xenopus oocytes. Identification of an ovalbumin signal sequence. J Mol Biol 180:645–666. https://doi.org/10.1016/0022-2836(84)90031-7.
31. Belin D, Wohlwend A, Schleuning WD, Kruithof EK, Vassalli JD. 1989. Facultative polypeptide translocation allows a single mRNA to encode the secreted and cytosolic forms of plasminogen activators inhibitor 2. EMBO J 8:3287–3294. https://doi.org/10.1002/j.1460-2075.1989.tb08489.x.
32. Rodenhuis-Zybert IA, van der Schaar HM, da Silva Voorham JM, van der Ende-Metselaar H, Lei HY, Wilschut J, Smit JM. 2010. Immature dengue virus: a veiled pathogen? PLoS Pathog 6:e1000718. https://doi.org/10.1371/journal.ppat.1000718.
33. Richards RM, Lowy DR, Schiller JT, Day PM. 2006. Cleavage of the papillomavirus minor capsid protein, L2, at a furin consensus site is necessary for infection. Proc Natl Acad Sci U S A 103:1522–1527. https://doi.org/10.1073/pnas.0508815103.
34. Pigors M, Sarig O, Heinz L, Plagnol V, Fischer J, Mohamad J, Malchin N, Rajpopat S, Kharfi M, Lestringant GG, Sprecher E, Kelsell DP, Blaydon DC. 2016. Loss-of-function mutations in SERPINB8 linked to exfoliative ichthyosis with impaired mechanical stability of intercellular adhesions. Am J Hum Genet 99:430–436. https://doi.org/10.1016/j.ajhg.2016.06.004.
35. DuBridge RB, Tang P, Hsia HC, Leong PM, Miller JH, Calos MP. 1987. Analysis of mutation in human cells by using an Epstein-Barr virus shuttle system. Mol Cell Biol 7:379–387. https://doi.org/10.1128/MCB.7.1.379.
36. Businger R, Kivimaki S, Simeonov S, Vavouras Syrigos G, Pohlmann J, Bolz M, Muller P, Codrea MC, Templin C, Messerle M, Hamprecht K, Schaffer TE, Nahnsen S, Schindler M. 2021. Comprehensive analysis of human cytomegalovirus- and HIV-mediated plasma membrane remodeling in macrophages. mBio 12:e0177021. https://doi.org/10.1128/mBio.01770-21.
37. Krapp C, Hotter D, Gawanbacht A, McLaren PJ, Kluge SF, Sturzel CM, Mack K, Reith E, Engelhart S, Ciuffi A, Hornung V, Sauter D, Telenti A, Kirchhoff

F. 2016. Guanylate binding protein (GBP) 5 is an interferon-inducible inhibitor of HIV-1 infectivity. Cell Host Microbe 19:504–514. https://doi.org/10.1016/j.chom.2016.02.019.
38. Sauter D, Schindler M, Specht A, Landford WN, Munch J, Kim KA, Votteler J, Schubert U, Bibollet-Ruche F, Keele BF, Takehisa J, Ogando Y, Ochsenbauer C, Kappes JC, Ayouba A, Peeters M, Learn GH, Shaw G, Sharp PM, Bieniasz P, Hahn BH, Hatziioannou T, Kirchhoff F. 2009. Tetherin-driven adaptation of Vpu and Nef function and the evolution of pandemic and nonpandemic HIV-1 strains. Cell Host Microbe 6:409–421. https://doi.org/10.1016/j.chom.2009.10.004.
39. Heusinger E, Kluge SF, Kirchhoff F, Sauter D. 2015. Early Vertebrate Evolution of the Host Restriction Factor Tetherin. J Virol 89:12154–12165. https://doi.org/10.1128/JVI.02149-15.
40. Parrish NF, Gao F, Li H, Giorgi EE, Barbian HJ, Parrish EH, Zajic L, Iyer SS, Decker JM, Kumar A, Hora B, Berg A, Cai F, Hopper J, Denny TN, Ding H, Ochsenbauer C, Kappes JC, Galimidi RP, West AP, Jr, Bjorkman PJ, Wilen CB, Doms RW, O'Brien M, Bhardwaj N, Borrow P, Haynes BF, Muldoon M, Theiler JP, Korber B, Shaw GM, Hahn BH. 2013. Phenotypic properties of transmitted founder HIV-1. Proc Natl Acad Sci U S A 110:6626–6633. https://doi.org/10.1073/pnas.1304288110.
41. Ochsenbauer C, Edmonds TG, Ding H, Keele BF, Decker J, Salazar MG, Salazar-Gonzalez JF, Shattock R, Haynes BF, Shaw GM, Hahn BH, Kappes JC. 2012. Generation of transmitted/founder HIV-1 infectious molecular clones and characterization of their replication capacity in CD4 T lymphocytes and monocyte-derived macrophages. J Virol 86:2715–2728. https://doi.org/10.1128/JVI.06157-11.
42. Connor RI, Chen BK, Choe S, Landau NR. 1995. Vpr is required for efficient replication of human immunodeficiency virus type-1 in mononuclear phagocytes. Virology 206:935–944. https://doi.org/10.1006/viro.1995.1016.
43. Wenigenrath J, Kolesnikova L, Hoenen T, Mittler E, Becker S. 2010. Establishment and application of an infectious virus-like particle system for Marburg virus. J Gen Virol 91:1325–1334. https://doi.org/10.1099/vir.0.018226-0.
44. Teufel F, Almagro Armenteros JJ, Johansen AR, Gislason MH, Pihl SI, Tsirigos KD, Winther O, Brunak S, von Heijne G, Nielsen H. 2022. SignalP 6.0 predicts all five types of signal peptides using protein language models. Nat Biotechnol 40:1023–1025. https://doi.org/10.1038/s41587-021-01156-3.